EPI International Journal of Engineering
Volume 2, Number 1, February 2019, pp. 28-33
DOI: 10.25042/epi-ije.022019.06

*p*ISSN 2615-5109
*e*ISSN 2621-0541

Heave and Pitch Motion Performances of a Ship Towing System Incorporated with Symmetrical Bridle Towline Model

Ahmad Fitriadhy[a,*], Nur Adlina Aldin[b], Nurul Aqilah Mansor[c], Nur Aqilah Hanis[d]

[a]Programme of Maritime Technology, School of Ocean Engineering, University Malaysia Terengganu. Email: naoe.afit@gmail.com
[b]Programme of Maritime Technology, School of Ocean Engineering, University Malaysia Terengganu. Email: nuradlina1910@gmail.com
[c]Programme of Maritime Technology, School of Ocean Engineering, University Malaysia Terengganu. Email: n.aqilahmansor@gmail.com
dProgramme of Maritime Technology, School of Ocean Engineering, University Malaysia Terengganu. Email: aqilahzaniza@gmail.com

Abstract

An investigation on vertical motion characteristics of a ship towing system incorporated with symmetrical bridle towline configuration set a real challenge for the naval architect engineer. This paper presents a Computational Fluid Dynamic (CFD) approach to analyse heave and pitch motion performances in waves. Several towing parameters such as various towline length and towing's velocity have been taken into account. Here, 1B (barge) is employed in the simulation; and designated as a towed ship. The results revealed that the subsequent increase of the towline lengths has been basically proportional with the increase of her heave motion; while inversely decrease in pitch motions. In addition, the effect of the extending towline length l' = 1.0 to 3.0 resulted in insignificant effect to the towline tension. However, the increase of the towing's velocity from 0.509 m/s to 0.728 m/s has led to significantly increase her heave motion and the towline tension by 40.46% and 24%, respectively; meanwhile, the pitch motion barge has sufficiently decreased by 35.94%. This simulation has been beneficial for the towing operator to ensure a higher level of the safety navigation of ship towing system.

Keywords: Bridle towline model; CFD; heave motion; pitch motion; towline tension

1. Introduction

Development of the global economics and drastic growth of shipping industries leads to heavy congestion due to abundant of ships in the waterways which threaten the safety of towed barge. Towing system is less course-keeping stable than the conventional single ships and it is dangerous when it runs in harsh environmental conditions. Therefore, an extensive investigation on towline tension is then required to observe the behaviour of towed barge using symmetrical bridle towline during towing operations.

Several researchers have attempted various approaches to investigate the performance of the ship towing system in calm water. Inoue et al [1], Lee [2], Kijima et al [3], Fitriadhy et al. [4] and Fitriadhy et al. [5] analysed the towed barge by numerical approaches. Lee [2] studied the tension of the towline using different material of towline, polyester and nylon while the effect of the towline length, tow point location on barge and tug proposed by Fitriadhy et al [4]. Experimental approach was conducted by Im et al [6] to investigate the effect of different towline configuration and employing active thruster to the barge. Im et al extended their research experiment using Computational Fluid Dynamics (CFD) for further validation.

Since numerical calculation and experiment have limitation in accurately reflecting the effect of interference and viscosity that affect the motion of vessel, CFD is employed to analyze the effects of nonlinearities, such as generation of 3D vortices [6]; computed the sway force and yaw moment during drift and steady yaw motion and analysed the flow field around the barge. Nonaka et al. [7] determine the fluid motion around the hull of a vessel and the hydrodynamics force exerted on a drifting vessel as well as presence of strong nonlinearities and complex flowfield [7]. CFD approach had been widely applied in maritime technology field such as estimating the vessel performance [8-10], resistance [11-15], and ship motions characteristics [16-21].

The assessment of ship motion characteristics is carried out in calm water conditions, but evaluation of ship in waves is more realistic since sea-going ships sails through waves. The effects of waves alter the water particle kinematics around the ship hydrodynamic forces acting on it, resulting in change of ship motions as stated by Rameesha and Krishnankutty in 2018. Hence, for the safety of towed barge during towing operations, it is important to include wave effects on the motion of barge to assess the motion of barge during ocean going towing. Waves from different headings particularly induce motion responses of the vessels and this may limit the

*Corresponding author. Tel.: +6-09-668-3350
Programme of Maritime Technology, School of Ocean Engineering, Universiti Malaysia Terengganu, 21030 Kuala Terengganu, Terengganu, Malaysia.

operability of the towing process [22]. Nam [22], Das [23] and Lee [24] studied the barge motion characteristics in waves using CFD approach. Their studies show that CFD can interpret turbulent free surface considering the viscosity and prove that the pressure changes around the barge affect the motion characteristics of the barge.

Thus, this paper presents a CFD simulation to predict heave and pitch motion performance of a ship towing system in waves incorporated with the symmetrical bridle towline configuration. Several effects such as towline length and towing's velocity have been mainly considered in the simulation. 1B (barge) is the symbol of the towed ship that employed in the simulation. Here, a commercial CFD so called Flow3D v11.2 is utilized by applying unsteady Reynolds-Averaged Navier Stokes Equation (RANSE). Flow3D incorporates different technique (TruVOF) to capture the free surface and computes flow variable only within one fluid. The heave and pitch motion performances are then clearly discussed.

2. Governing Equation

The CFD flow solver on FLOW-3D version 11.2 is based on the incompressible unsteady RANS equations in which the solver applies the Volume of Fluid (VOF) to track the free surface elevation. The interface between fluid and solid boundaries is simulated with the fractional area volume obstacle representation favor method. This method computes open area and volume in each cell to define the area that is occupied by obstacle.

2.1. Continuity and momentum equation

The continuity and momentum equations for a moving object and the relative transport equation for VOF function are

$$\frac{V_f}{\rho}\frac{\partial \rho}{\partial t} + \frac{1}{\rho}\nabla.\left(\rho \vec{u} A_f\right) = -\frac{\partial V_f}{\partial t} \tag{1}$$

$$\frac{\partial \vec{u}}{\partial t} + \frac{1}{V_f}\left(\vec{u} A_f.\nabla \vec{u}\right) = -\frac{1}{\rho}\left[\nabla_\rho + \nabla.\left(\tau A_f\right)\right] + \vec{G} \tag{2}$$

$$\frac{\partial F}{\partial t} + \frac{1}{V_f}\nabla.\left(F \vec{u} A_f\right) = -\frac{F}{V_f}\frac{\partial V_f}{\partial t} \tag{3}$$

where ρ is the density of the fluid, $\vec{u}$ is the fluid velocity, V_f is the volume fraction, A_f is the area fraction, p is the pressure, τ is the viscous stress tensor, G denotes gravity and F is the fluid fraction.

In the case of coupled GMO's motion, Eqs.(1) and (2) are solved at each time step and the location of all moving objects is recorded and the area and volume fractions updated using the FAVOR technique. Equations (3) are solved with the source term $\left(-\frac{\partial V_f}{\partial t}\right)$ on the right-hand side which is computed as

$$-\frac{\partial V_f}{\partial t} = \vec{U}_{obj}\vec{n}S_{obj}/\,V_{cell} \tag{4}$$

where S_{obj} is the surface area, $\vec{n}$ surface normal vector, $\vec{U}_{obj}$ is the velocity of the moving object at a mesh cell and V_{cell} is the total volume of the cell [25].

2.2. Turbulence model

The RNG turbulence model was used for the simulation of the exchange flow between open water and floating object since it accounts for low Reynolds number effects [26-28]. Applying the double averaging strategy to the transport equations for TKE and its dissipation rate produces the turbulence model for the flow. The resulting equations are:

$$\frac{\delta k}{\delta t} + U_j\frac{\delta k}{\delta x_j} = \frac{\delta}{\delta x_j}\left[\left(v + \frac{v_t}{\sigma_k}\right)\frac{\delta k}{\delta x_j}\right] + P_k + B_k + W_k \tag{5}$$

$$\frac{\delta \varepsilon}{\delta t} + U_j\frac{\delta \varepsilon}{\delta x_j} = \frac{\delta}{\delta x_j}\left[\left(v + \frac{v_t}{\sigma_\varepsilon}\right)\frac{\delta \varepsilon}{\delta x_j}\right] + C_{1\varepsilon}\frac{\varepsilon}{k}(P_k + B_k)(1 + C_{3\varepsilon}R_f) + W_\varepsilon - C^*_{2\varepsilon}\frac{\varepsilon^2}{k} \tag{6}$$

$$P_k = v_t S^2 = v_t\left(\frac{\delta U_i}{\delta x_j} + \frac{\delta U_j}{\delta x_i}\right)\frac{\delta U_i}{\delta x_j} \tag{7}$$

$$B_k = \beta g_i \frac{v_t}{\sigma_s}\frac{\delta s}{\delta x_i} \tag{8}$$

where P_k is the shear production term of TKE, $S = \sqrt{2S_{ij}S_{ji}}$ is the modulus of the mean rate of strain tensor and $S_{ij} = \frac{1}{2}\left(\frac{\delta U_i}{\delta x_j} + \frac{\delta U_j}{\delta x_i}\right)$, B_k is the buoyant production term of TKE, W_k is the wake production tern of TKE, W_ε is the wake production term in ε, σ_k and σ_ε are the turbulent Prandtl numbers for k and ε, and $C_{i\varepsilon}$, $C_{3\varepsilon}$ and $C^*_{2\varepsilon}$ are model coefficients.

2.3. Body motion equation

The body motion was analysed in a space-fixed Cartesian coordinate system, the global coordinate system. The governing equation of the six degree of freedom (DOF) of a rigid body motion can be expressed in this coordinate system as

$$\frac{d}{dt}(m\vec{v}_c) = \vec{f} \tag{9}$$

$$\frac{d}{dt}(M_c.\vec{w}_c) = \vec{m}_c \tag{10}$$

The index C denotes the centre of mass of the body, m denotes the mass of the body, $\vec{v}_c$ the velocity vector, M_c is the tensor of the moments of inertia, $\vec{\omega}_c$ is the angular velocity vector, $\vec{f}$ denotes the resulting force vector and $\vec{m}_c$ denotes the resultant moment vector acting on the body [12]. The resultant force $\vec{f}$ has three components; surface force, field forces and external forces:

$$\vec{f} = \int_S (T - \rho I).\vec{n}dS + \int_V \rho_b \vec{b}dV + \vec{f}E \tag{11}$$

Here, ρ_b is the density of the body. The only field force considered is the gravity, so the volume integral of above equation (right hand side) reduces to $m\vec{g}$, where g is the gravity acceleration vector. The vector $f\vec{E}$ denotes the external forces acting in the body [29].

2.4. Waves

The model is based on Airy's linear wave theory. The linear wave is assumed to come from flat bottom reservoir into the computational domain [30]. The linear wave theory is based on the following assumptions; fluid is incompressible, inviscid, irrational, two-dimensional flow and the wave amplitude (A) is small compared to the mean water depth (h) and wavelength (λ). With the assumption, the problem can be reduced to a linear potential flow problem. The free surface elevation $\eta(x,t)$ measured in the vertical direction from mean water surface, the velocity potential $\varphi(x,z,t)$ and velocity components in x and z directions $u(x,z,t)$ and $w(x,z,t)$ are obtained as

$$\eta = A\ \cos(kx - \omega t + \phi) \tag{12}$$

$$\varphi(x,z,t) = xU + \frac{A\omega\cosh[k(z+h)]\sin(kx-\omega t+\phi)}{k\sinh(kh)} \tag{13}$$

$$u(x,z,t) = U + \frac{A\omega\cosh[k(z+h)]\cos(kx-\omega t+\phi)}{\sinh(kh)} \tag{14}$$

$$w(x,z,t) = \frac{A\omega\sinh[k(z+h)]\sin(kx-\omega t+\phi)}{\sinh(kh)} \tag{15}$$

where ϕ is the phase shift angle, t is time.

The dispersion equation in terms of wave speed $c = \omega/k$ is given by

$$(c-U)^2 = \frac{g}{k}\tanh(kh) \tag{16}$$

3. Simulation Conditions

The CFD flow solver on FLOW-3D version 11.2 is based on the incompressible unsteady RANS equations in which the solver applies the Volume of Fluid (VOF) to track the free surface elevation. The interface between fluid and solid boundaries is simulated with the fractional area volume obstacle representation favor method. This method computes open area and volume in each cell to define the area that is occupied by obstacle.

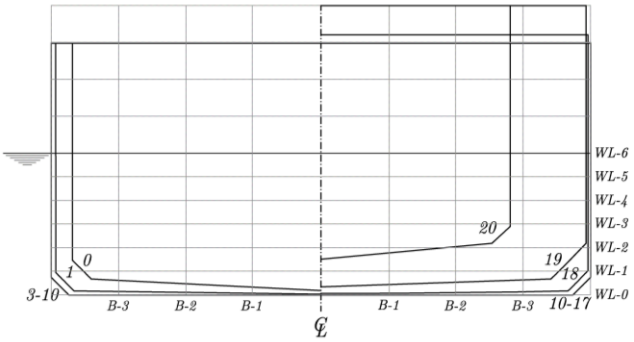

Figure 1. Body plan of barge

Table 1. Principal dimensions of barge (1B)

Description	1B	
	Full-scale	Model
Length, *L(m)*	60.96	1.219
Breadth, *B(m)*	10.67	0.213
Draft, *d(m)*	2.74	0.0548
Volume, $V(m^3)$	1646.2	0.01317
L/B	5.71	5.71
Block coefficient,C_b	0.92	0.92
k_{yy2}/L	0.3266	0.3266
$X_{G\ abaft\ the\ midship}$,*(m)*	-1.04	-0.0208

Table 2. Various towline length, l'

Towing velocity, V_s (m/s)	Towline length, l'	Wavelength, λ/lpp
	1.0	
0.509	2.0	1.0
	3.0	

3.1. Principal data of ships

The principal dimensions barge (1B) are presented in Table 1. Her respective body plan is shown in Fig.1.

3.2. Parametric studies

Table 2 presents various towline length employed in the simulations. Towing's velocity, V_s is kept constant by 0.509 m/s. Various towing's velocity, V_s used in the simulation are shown in Table 3 with fixed towline length, l'=1.0 L. Towing point location is set to l'_b=0.5 for both cases.

Table 3. Various towing's velocity, V_s.

Towing velocity, V_s (m/s)	Towline length, l'	Wavelength, λ/lpp
0.509		
0.582	1.0	1.0
0.655		
0.728		

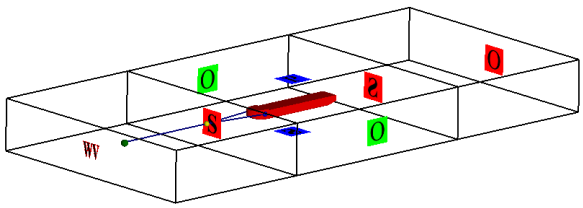

Figure 2. Boundary conditions

Table 4. Various towing's velocity, V_s.

Boundary	Mesh block 1	Mesh block 2
X_{min}	Wave	Symmetry
X_{max}	Outflow	Symmetry
Y_{min}	Outflow	Symmetry
Y_{max}	Outflow	Symmetry
Z_{min}	Symmetry	Symmetry
Z_{max}	Specified pressure	Symmetry

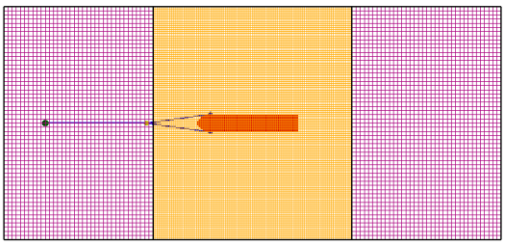

Figure 3. Meshing generation

3.3. Computational domain and boundary conditions

The computational domain uses a structured mesh that is defined in a Cartesian. Referring to Fig.2, the boundary condition is mark in the mesh block 1 and mesh block 2. The boundary condition at X-max boundary is wave, linear wave so that there is wave generated into the simulation. In order to save computational time, wave is assigned to water at X-max boundary. As for X-min, Y-max and Y-min boundary, outflow is assigned to prevent reflection while Z-min is symmetry and Z-max is specified pressure. The boundary conditions for this simulation are shown in Table 4.

The meshing generation is created in Flow3D v11.2 as shown in Fig.3. An extra refinement of the mesh called nested block is added to increase meshing resolution in this study. The barge is coupled through a towline. A virtual tug, a sphere model is assigned prescribed motion while barge as towed ship was set as coupled motion in X-translational, Z-translational and Y-rotational motions (surge, heave and pitch motions). The barge was in 5° inclination arrangement initially. The towline is set as polyester mooring line with spring coefficient of 7.347 N/m^2.

Based on the applications of Flow3D v11.2, the average duration of every simulation was about 70-80 hours (4 parallel computations) on a HP Z820 workstation PC with processor Intel (R) Xeon (R) CPU ES-2690 v2 @ 3.00 GHz (2 processors) associated with the installed memory (RAM) of 32.0 GB and 64-bit Operating System.

4. Results and Discussions

Referring to Figs.4-7, the CFD simulation has been successfully carried out to predict the course stability of the towing system in various towline lengths and towing's velocity. The simulations results of heave and pitch motion performances of the barge associated with the towline tension are presented.

4.1. Effect of various towline lengths

The characteristics of heave and pitch motion characteristics at various towline lengths have been displayed in Fig.4. Here, the extending towline length from l' = 1.0 to 3.0 resulted in the increase of the heave motion of the barge by 17.7%; meanwhile her pitch motion decreased 7.4%. This could be explained the CFD simulation that the free surface elevation around the barge subsequently increased, which indicated by high pressure region (red color) as the towline extended up l' = 3.0. However, this extending towline was insignificant to the increase of the maximum towline tension about 8.5% as the increase the towline from l' = 1.0 to 2.0.

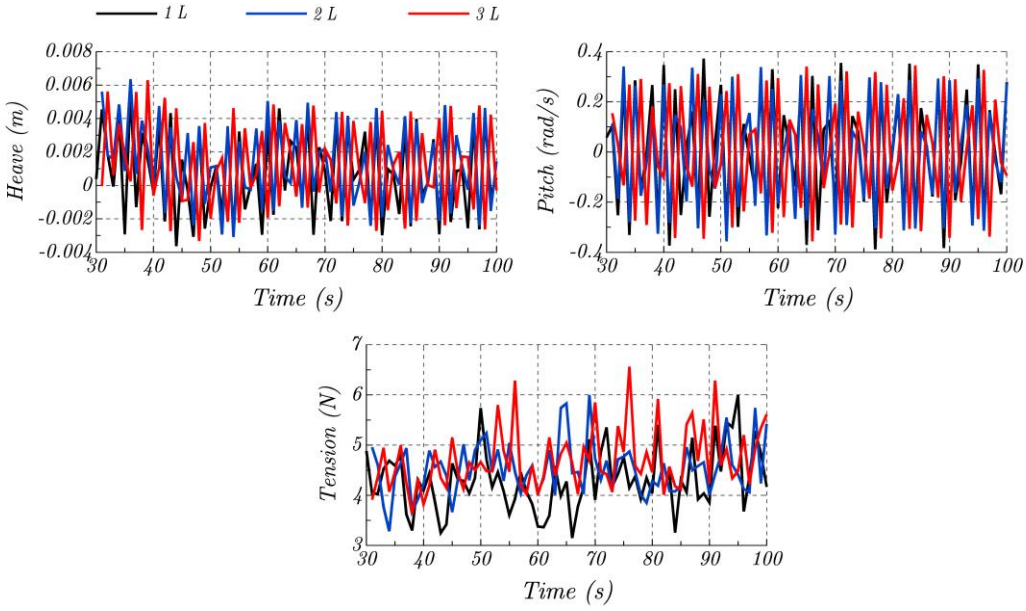

Figure 4. Characteristics of heave and pitch motion of 1B associated with the towline tension at various towing's velocity

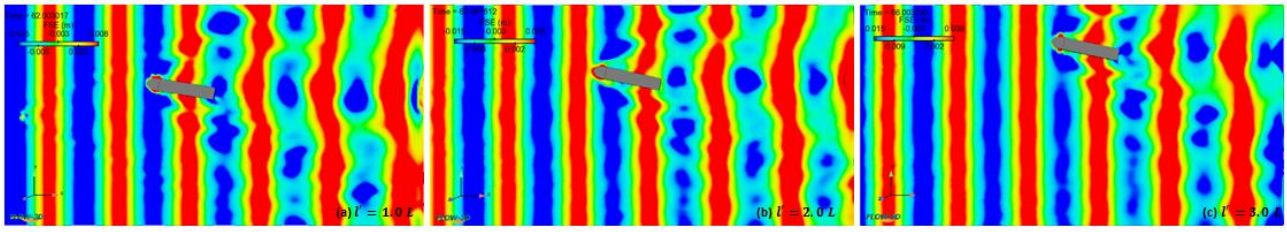

Figure 5. Free surface elevation, V_s= 0.509 m/s, l'=1.0 (a), 2.0 (b) and 3.0 (c)

4.2. Efect of various towing's velocity

The characteristics of heave and pitch motion performances with the symmetrical bridle towline model associated with dynamic towline tension in various towing's velocity have been displayed in Figure 6. The subsequent increase of the towing's velocity from V_s =0.509 to 0.582 m/s and 0.655 m/s to 0.728 m/s resulted in the increment of heave motion by 24% and 29.9%, respectively. However, the pitch motion of the barge decreased by 35.9% as towing's velocity increased from V_s = 0.509 m/s to 0.728 m/s; meanwhile the towline tension increased by 24%. This can be explained by the CFD simulation (see Figure 7) that the heave motions at the maximum towing's velocity of 0.728 m/s has been the highest ones due to the higher pressure phenomenon indicated by the subsequent increase of the red color at the aft region as compared to the towing velocity of 0.582 m/s and 0.655 m/s. On the other hand, the effects of resonance and exciting forces due to the incoming waves have also contributed to the increase of the larger vertical motion responses of the barge (the towed ship) [20].

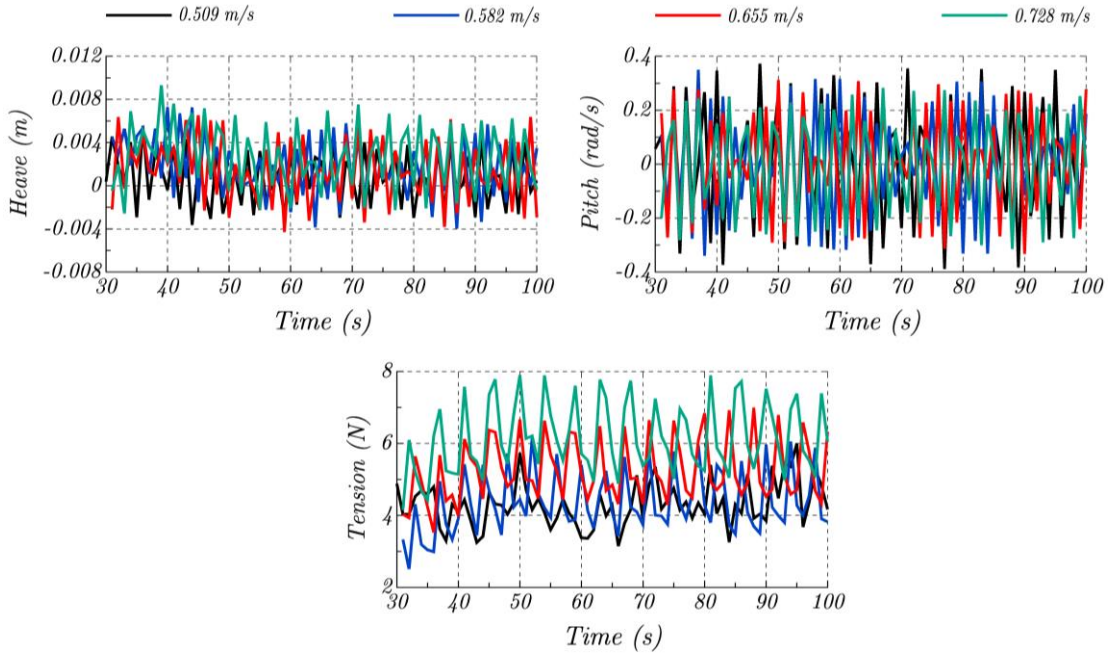

Figure 6. Characteristics of heave and pitch motion of 1B associated with the towline tension at various towing's velocity

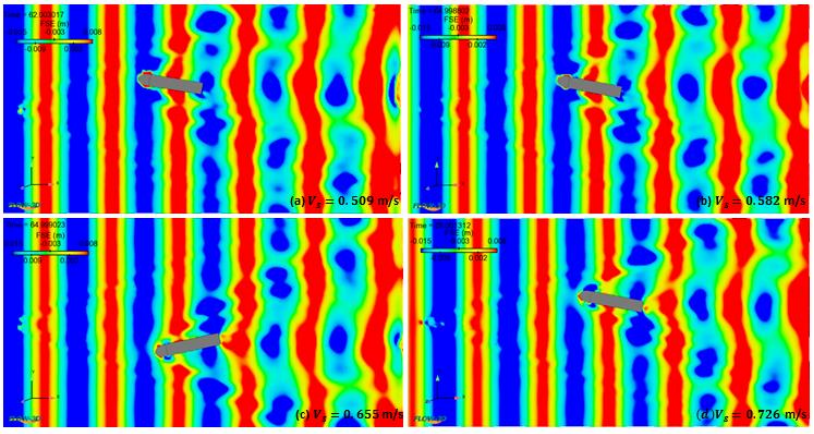

Figure 7. Free surface elevation , l'=1.0, V_s= 0.509 m/s (a), 0.582 m/s (b) 0.655 m/s (c) and 0.728 m/s (d)

5. Conclusions

The Computational Fluid Dynamics (CFD) analysis on the heave and pitch motion characteristics of barge incorporated with the symmetrical towline model has been successfully performed using Flow3D v11.2 software. The effect of various towline length and towing's velocity have taken into the simulation. The simulations results can be drawn as follow:

- Basically, the extending towline length from l' = 1.0 to 3.0 results in the increase of the heave motion of the barge by 17.7%; while her pitch motion decreases by 7.4%. It should be merely noted here that the towline tension exhibits insignificant effect when the towline length increases.
- The effect of the towing velocity has led to increase the heave motion of the barge by 40.46%; and inversely decreases her pitch motion by 35.94% as the towing velocity increases from 0.582 m/s to 0.728 m/s; meanwhile, the towline tension increases by 24%.

Refrences

[1] Inoue, S., Hirano, M. and Mukai, K. (1979). *The Nonlinear Terms of Lateral Force and Moment Acting on Ship Hull in the Case of Manoeuvering*. Trans. West-Japan Soc. Nav. Archit(58).

[2] Lee, M.-L. (1989). *Dynamic Stability of Nonlinear Barge-towing System*. Applied mathematical modelling, 13(12), 693-701.

[3] Kijima, K., Katsuno, T., Nakiri, Y. and Furukawa, Y. (1990). *On the manoeuvring performance of a ship with theparameter of loading condition*. Journal of the Society of Naval Architects of Japan, 1990(168), 141-148.

[4] Fitriadhy, A. and Yasukawa, H. (2011). *Course Stability of a Ship Towing System*. Ship Technology Research, 58(1), 4-23.

[5] Fitriadhy, A., Yasukawa, H., Wan Nik, W.B. and Abu Bakar, A. (2016). *Numerical Simulation of Predicting Dynamic Towline Tension on a Towed Marine Vehicle*. International Conference on Ships and Offshore Structures ICSOS 2016 31 August - 2 September 2016, Hamburg, Germany.

[6] Im, N., Lee, S. and Lee, C. (2015). *The influence of skegs on course stability of a barge with a different configuration*. Ocean Engineering, 97, 165-174.

[7] Nonaka, K., Fuwa, T. and Nimura, T. (1986). *Measurement of wake flow and hydrodynamic force distribution on a ship model with drift angle (2nd report, Tanker model)*. J. Soc. Naval Architects of West Japan, 72, 197-212.

[8] van Oers, B. and Toxopeus, S. (2006). *On the relation between flow behaviour and the lateral force distribution acting on a ship in oblique motion*. 10th International Cooperation on Marine Engineering Systems ICMES, London, UK.

[9] Miyazaki, H., Ueno, M. and Tsukada, Y. *Numerical study about effects of stern skeg on course stability*. in *The Twenty-first International Offshore and Polar Engineering Conference*. 2011. International Society of Offshore and Polar Engineers.

[10] Broglia, R., Dubbioso, G., Durante, D. and Di Mascio, A. (2013). *Simulation of turning circle by CFD: Analysis of different propeller models and their effect on manoeuvring prediction*. Applied Ocean Research, 39, 1-10.

[11] Tezdogan, T., Demirel, Y.K., Kellett, P., Khorasanchi, M., Incecik, A. and Turan, O. (2015). *Full-scale Unsteady RANS CFD Simulations of Ship Behaviour and Performance in Head Seas due to Slow Steaming*. Ocean Engineering, 97, 186-206.

[12] Maki, K.J., Broglia, R., Doctors, L.J. and Di Mascio, A. (2013). *Numerical investigation of the components of calm-water resistance of a surface-effect ship*. Ocean Engineering, 72, 375-385.

[13] Fitriadhy, A., Jamaluddin, A., Norsani, W.M., Wan Nik, W.B., Bakar, A., Azlan, M. and W. M. Noor, C. (2014). *Frictional Resistance's Prediction of a Trimaran Ship in Calm Water using Computational Fluid Dynamic (CFD) Approach*.

[14] Fitriadhy, A., Lim, P.S. and Jamaluddin, A., *CFD Investigation on Total Resistance Coefficient of Symmetrical and Staggered Catamaran Configurations through Quantifying Existence of an Interference Factor*, in *The First International Conference on Ships and Offshore Structures ICSOS 2016*. 2016: Hamburg, Germany. p. 1-20.

[15] Fitriadhy, A., Azmi, S., Mansor, N.A. and Aldin, N.A. (2017). *Computational fluid dynamics investigation on total resistance coefficient of a high-speed" deep-V" catamaran in shallow water*. International Journal of Automotive and Mechanical Engineering, 14, 4369-4382.

[16] Tezdogan, T., Incecik, A. and Turan, O. (2016). *A Numerical Investigation of the Squat and Resistance of Ships Advancing through a Canal using CFD*. Journal of marine science and technology, 21(1), 86-101.

[17] Sadat-Hosseini, H., Kim, D.-H., Carrica, P.M., Rhee, S.H. and Stern, F. (2016). *URANS simulations for a flooded ship in calm water and regular beam waves*. Ocean Engineering, 120, 318-330.

[18] Cercos-Pita, J.L., Bulian, G., Pérez-Rojas, L. and Francescutto, A. (2016). *Coupled simulation of nonlinear ship motions and a free surface tank*. Ocean Engineering, 120, 281-288.

[19] Zhang, G., Zhang, X. and Pang, H. (2015). *Multi-innovation auto-constructed least squares identification for 4 DOF ship manoeuvring modelling with full-scale trial data*. ISA transactions, 58, 186-195.

[20] Fitriadhy, A. and Adam, N.A. (2017). *Heave and pitch motions performance of a monotricat ship in head-seas*. International Journal of Automotive and Mechanical Engineering, 14, 4243-4258.

[21] Fitriadhy, A., Razali, N. and AqilahMansor, N. (2017). *Seakeeping performance of a rounded hull catamaran in waves using CFD approach*. Journal of Mechanical Engineering and Sciences, 11(2), 2601-2614.

[22] Nam, B.W., Kim, Y. and Hong, S.Y. (2015). *Hydrodynamic interaction between two barges during berthing operation in regular waves*. Ocean Engineering, 106, 317-328.

[23] Das, S., Das, S.K. and Kariya, J. (2012). *Simulation of return flow in restricted navigation channel for barge-tow movements*. Open Ocean Engineering Journal, 5, 34-46.

[24] Lee, S.-M., Jeong, U.-C. and Kim, H.-S. (2010). *Study on the Flow Characteristics around a Barge in Still Water*. Journal of Navigation and Port Research, 34(6), 417-422.

[25] *FLOW-3D 10.1.1 User Manual*. (2013). Flow Science Inc.

[26] Yakhot, V. and Orszag, S.A. (1986). *Renormalization group analysis of turbulence. I. Basic theory*. Journal of scientific computing, 1(1), 3-51.

[27] Yakhot, A., Rakib, S. and Flannery, W. (1994). *Low-Reynolds number approximation for turbulent eddy viscosity*. Journal of scientific computing, 9(3), 283-292.

[28] Koutsourakis, N., Bartzis, J.G. and Markatos, N.C. (2012). *Evaluation of Reynolds stress, k-ε and RNG k-ε turbulence models in street canyon flows using various experimental datasets*. Environmental fluid mechanics, 1-25.

[29] Yan, S. and Huang, G. (1996). *Dynamic Performance of Towing System-Simulation and Model Experiment*. Proceedings, OCEAN, 96.

[30] *Flow3D 10.1.1 User Manual*. (2013). Flow Science Inc.